

LETTER TO THE EDITOR

The Gaia-ESO Survey: Discovery of a spatially extended low-mass population in the Vela OB2 association^{★,★★}

G. G. Sacco¹, R. D. Jeffries², S. Randich¹, E. Franciosini¹, R. J. Jackson², M. Cottaar³, L. Spina¹, F. Palla¹, M. Mapelli⁴, E. J. Alfaro⁵, R. Bonito^{6,7}, F. Damiani⁷, A. Frasca⁸, A. Klutsch⁸, A. Lanzafame⁹, A. Bayo¹⁰, D. Barrado¹¹, F. Jiménez-Esteban^{11,12}, G. Gilmore¹³, G. Micela⁷, A. Vallenari⁴, C. Allende Prieto¹⁴, E. Flaccomio⁷, G. Carraro¹⁵, M. T. Costado⁵, P. Jofré¹³, C. Lardo¹⁶, L. Magrini¹, L. Morbidelli¹, L. Prisinzano⁶, and L. Sbordone¹⁷

(Affiliations can be found after the references)

ABSTRACT

The nearby (distance~350-400 pc), rich Vela OB2 association, includes γ^2 Velorum, one of the most massive binaries in the solar neighbourhood and an excellent laboratory for investigating the formation and early evolution of young clusters. Recent Gaia-ESO survey observations have led to the discovery of two kinematically distinct populations in the young (10-15 Myr) cluster immediately surrounding γ^2 Velorum. Here we analyse the results of Gaia-ESO survey observations of NGC 2547, a 35 Myr cluster located two degrees south of γ^2 Velorum. The radial velocity distribution of lithium-rich pre-main sequence stars shows a secondary population that is kinematically distinct from and younger than NGC 2547. The radial velocities, lithium absorption lines, and the positions in a colour-magnitude diagram of this secondary population are consistent with those of one of the components discovered around γ^2 Velorum. This result shows that there is a young, low-mass stellar population spread over at least several square degrees in the Vela OB2 association. This population could have originally been part of a cluster around γ^2 Velorum that expanded after gas expulsion or formed in a less dense environment that is spread over the whole Vela OB2 region.

Key words. Stars: formation – Stars: pre-main sequence – Techniques: spectroscopic – open clusters and association: Vela OB2 – open clusters and association: NGC 2547 – Stars: individual: γ^2 Velorum

1. Introduction

Observations of star forming regions (SFRs) in the solar neighbourhood show that very young stars can be found in both high-density, gravitationally-bound clusters and low-density, loose stellar associations (e.g., Carpenter 2000; Lada & Lada 2003). The origin of these young stellar populations is still being debated. All stars could form in massive dense clusters that expand to a larger volume after gas expulsion due to stellar winds, radiation pressure, and supernova explosions (e.g., Goodwin & Bastian 2006; Baumgardt & Kroupa 2007). Alternatively, stars may form in a wide range of environments, from the dense cores of massive clusters to sparse associations (Bressert et al. 2010; Wright et al. 2014). High-resolution spectroscopic surveys of SFRs and young clusters are powerful tools for investigating this topic, since stellar radial velocities (RVs) allow us to characterize their current dynamical state, establishing whether a SFR is bound or expanding into the field (e.g., Cottaar et al. 2012a; Jeffries et al. 2014), and for identifying and disentangling multiple populations seen in the same line of sight (e.g., Jeffries et al. 2006b; Alves & Bouy 2012).

The Vela OB2 association consists of 93 early-type stars selected using *Hipparcos* proper motions by de Zeeuw et al. (1999), which are distributed over an area of ~ 180 deg². The

mean Hipparcos distance to the Vela OB2 stars is 410 ± 12 pc, but its most massive star, γ^2 Velorum, is closer according to two interferometric observations of its orbit (336_{-7}^{+8} pc, North et al. 2007; 368_{-13}^{+38} pc, Millour et al. 2007). The association is surrounded by a dust shell of radius ~ 7.5 deg, centred on γ^2 Velorum, which is probably powering its expansion (Sahu 1992; Pettersson 2008). Recently, the young cluster (hereafter, the Gamma Vel cluster) around γ^2 Vel has been observed by the Gaia-ESO Survey (Gilmore et al. 2012; Randich & Gilmore 2013). The results of these observations, covering about one square degree around the massive binary, are discussed in Jeffries et al. (2014). They found that the cluster is composed of two kinematically distinct populations, which are older than previously thought (≥ 10 Myr) and have an age difference of $\sim 1-2$ Myr. The older population (Gamma Vel A) is more concentrated around γ^2 Vel and is roughly in virial equilibrium, while the younger population (Gamma Vel B) is extended, clearly unbound, and supervirial; namely, the total kinetic energy of the cluster is higher than in a bound system in equilibrium.

The cluster NGC 2547 (RA = 08h10m, DEC=-49d12m) is located about two degrees south of γ^2 Vel (~ 10 pc at the distance of γ^2 Vel). Several distance estimates, from 360–480 pc, are available in the literature (Claria 1982; Shobbrook 1986; Lyra et al. 2006; Naylor & Jeffries 2006; van Leeuwen 2009). An accurate age of 35 ± 3 Myr has been derived from the lithium-depletion boundary (Jeffries & Oliveira 2005). The Gaia-ESO cluster targets are selected to well sample the age-distance-position parameter space. NGC2547 is particularly important given its age (one of the few clusters with an age between 10

* Based on observations made with the ESO/VLT, at Paranal Observatory, under program 188.B-3002 (The Gaia-ESO Public Spectroscopic Survey)

** Table 1 is only available at CDS via anonymous ftp to cdsarc.u-strasbg.fr (130.79.128.5) or via <http://cdsweb.u-strasbg.fr/cgi-bin/qcat?J/A+A/>

and 50 Myr) and relatively short distance to the Sun. Here, we report the discovery of a secondary population that is younger and kinematically distinct from NGC 2547. We show that this second component has a similar age to Gamma Vel B and is kinematically indistinguishable from it, providing evidence for a very extended low-mass component of the Vela OB2 association.

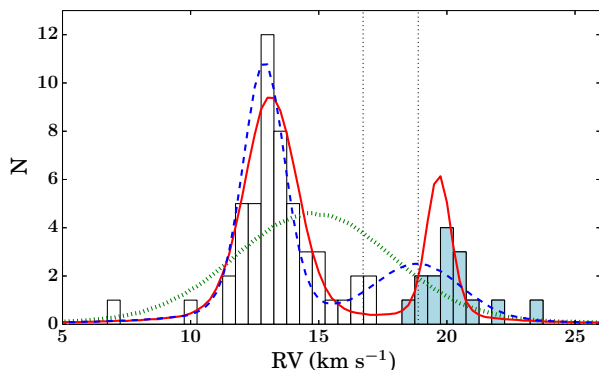


Fig. 1. RV distribution for all the stars with $\text{EW}(\text{Li}) > 100 \text{ m}\text{\AA}$. The three lines describe the best-fit models obtained using: (a) one stellar population with a Gaussian distribution (green dotted line), (b) one population with a Gaussian distribution and a second one with the same distribution of Gamma Velorum B (blue dashed line), and (c) two populations with Gaussian distributions (red continuous line). Stars with > 80 per cent probability of belonging to population B according to model (b) are highlighted with blue shading. The vertical dotted black lines indicate the central velocity of Gamma Vel A (left) and Gamma Vel B (right) found by Jeffries et al. (2014).

2. Observations and data

The Gaia-ESO survey observations (see Gilmore et al. 2012; Randich & Gilmore 2013) were carried out with the multi-object optical spectrograph FLAMES at the VLT, composed of a robotic fibre positioner feeding the GIRAFFE ($R \sim 17,000$) and UVES ($R \sim 47,000$) spectrographs, with 132 and 8 fibres respectively (Pasquini et al. 2002).

In this paper, we only use GIRAFFE data. The GIRAFFE candidate members are selected using a common strategy discussed in Bragaglia et al. (in prep.). Specifically, for NGC 2547 we used a two-step process: 1) we identified the regions including all the known cluster members in optical colour-magnitude diagrams (CMDs), using optical photometric data in the literature (Naylor et al. 2002; Jeffries et al. 2004) and a catalogue of members based on X-ray observations (Jeffries et al. 2006a); 2) we selected all stars in these regions with $11 < V < 19$ (or $10.5 < I < 16$ in the absence of V photometry). The selected catalogue of candidate cluster members includes 467 stars distributed over an area of about 1 deg^2 . We observed 450 candidates in 16 FLAMES fields (diameter $\sim 25 \text{ arcmin}$ each) with GIRAFFE, during two separate runs in January and February 2013. Many stars were included in two or more overlapping fields and observed multiple times. In each field at least 20 fibres were used to acquire sky background spectra. All the observations were performed with the HR15N filter covering 647–679 nm. Exposure times were 1200 or 3000 s, depending on the brightness of the targets.

The survey spectra were processed and analysed by 20 working groups organized in a workflow, that is described in Gilmore et al. (2012). GIRAFFE spectra were reduced with a pipeline developed at the Cambridge Astronomical Survey Unit,

which also calculates radial velocities (RVs) and projected rotation velocities. A more detailed description of the data reduction and an assessment of the accuracy and the precision of the RVs is given in Jeffries et al. (2014) and Lewis et al. (in prep.). The reduced spectra of young stars were analysed by a dedicated working group composed of several teams, which derive the stellar parameters (effective temperatures, gravities, chemical abundances, accretion tracers, as well as equivalent widths of the $\text{Li I } 670.8 \text{ nm}$ line – $\text{EW}(\text{Li})$). The final parameters are weighted means of the results provided by the teams after outliers are rejected. A detailed description of the methods used and a discussion of accuracy and precision are given by Lanzafame et al. (2015). The data presented in this paper are part of the second internal data release (GESviDR2) of July 2014 and are reported in Table 1, which is available at the CDS.

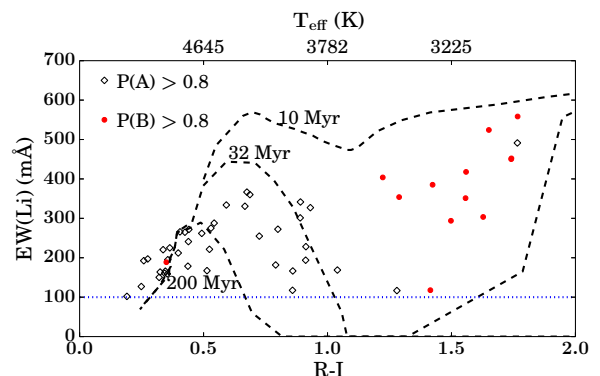


Fig. 2. Equivalent width of Li 670.8 nm absorption as a function of $R-I$ (corrected for the extinction $E(B-V) = 0.06$ derived by Claria 1982) for stars with > 80 per cent probability of belonging to population A (empty diamonds) or population B (red circles). The black dashed lines are isochrones of Li depletion calculated from the Baraffe et al. (1998) models at 10, 32, and 200 Myr, and the horizontal dotted blue line indicates the threshold used to select the pre-main sequence stars. The x-axis on the top of the panel reports a scale of effective temperature derived from $R-I$ using the Pecaut & Mamajek (2013) colour-temperature transformations.

3. Population B of NGC 2547

The strategy for the selection of targets for young clusters in the Gaia-ESO Survey is tailored to observe an unbiased and nearly complete sample, but can lead to significant contamination by field stars (e.g., Jeffries et al. 2014). To cleanly study the kinematics of the young NGC 2547 population and search for additional young populations, we need to remove these contaminants.

Since pre-main sequence (PMS) stars with $T_{\text{eff}} \sim 4000 \text{ K}$ completely deplete their photospheric lithium in $\leq 100 \text{ Myr}$ (Siess et al. 2000; Baraffe et al. 1998), a filtered sample can be created by excluding all stars with no evidence of Li absorption at 670.8 nm. This approach isolates a sample of young stars at cool temperatures, but will not select all members of NGC 2547, since many M-type PMS stars at an age of 35 Myr will also have depleted their lithium (Jeffries & Oliveira 2005).

Figure 1 shows the RV distribution of all the observed stars with $\text{EW}(\text{Li}) > 100 \text{ m}\text{\AA}$. The distribution is characterized by two peaks at $\sim 13 \text{ km s}^{-1}$ and $\sim 20 \text{ km s}^{-1}$, respectively. The position of the former and most prominent peak is consistent with the mean RV of NGC 2547 ($12.8 \pm 1 \text{ km s}^{-1}$) derived by Jeffries et al. (2000), while none of the previous spectroscopic studies of this

Table 1. Results from maximum likelihood modelling of the radial velocities.

	One component	One component+ γ Vel B	Two components
RV_A (km s $^{-1}$)	14.68 ± 0.44 (14.79)	12.94 ± 0.17 (12.87)	13.05 ± 0.21 (13.13)
σ_A (km s $^{-1}$)	3.07 ± 0.36 (2.95)	0.83 ± 0.17 (0.74)	0.97 ± 0.23 (0.95)
RV_B (km s $^{-1}$)		18.88	18.9 ± 0.95 (19.68)
σ_B (km s $^{-1}$)		1.6	1.83 ± 1.40 (0.61)
f_A	1.00	0.69 ± 0.06 (0.70)	0.72 ± 0.09 (0.75)
$\ln(L_{max})$	-194.9	-174.6	-173.81

Notes. Symmetric 68 per cent confidence intervals for one parameter of interest, the value at the maximum likelihood is given in parentheses. The parameters RV_A , RV_B , σ_A and σ_B represent the mean and the standard deviation of the normal distributions describing the intrinsic RV distributions of the single stars in population A and B. The parameter f_A is the fraction of stars belonging to population A, while $\ln L_{max}$ is the maximum log-likelihood of the fits.

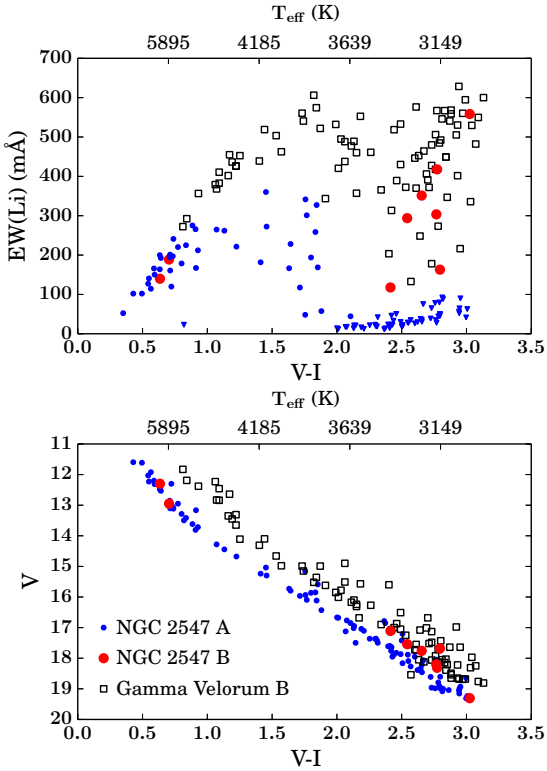


Fig. 3. Comparison between the multiple populations discovered in NGC 2547 and Gamma Vel B. The top panel shows the EW(Li) as a function of $V - I$, while the bottom panel shows a V vs $V - I$ CMD. Photometry has been corrected according to the extinction towards NGC2547 ($E(B-V)=0.06$) and Gamma Velorum ($E(B-V)=0.055$). The x-axis on the top reports an effective temperature scale derived from $V-I$, using the colour-temperature transformations described in Pecaut & Mamajek (2013). In both panels empty squares, filled red circles, and blue circles indicate the stars of Gamma Vel B, NGC 2547 B, and NGC 2547 A respectively. EW(Li) upper limits in NGC 2547 A are reported with downward triangles. Only a subsample of stars of NGC 2547 is shown, since V band photometry is not available for all targets (see footnote on page 4).

cluster mention a kinematically distinct secondary population with very similar velocity to Gamma Vel B (18.9 ± 0.5 km s $^{-1}$ from Jeffries et al. 2014). To test the hypothesis that the population associated with the second RV peak (called NGC2547 B in the rest of the paper) and Gamma Vel B have the same origin, we model the RV distribution shown in Fig. 1 using the same maximum likelihood technique as described in detail in Jeffries et al.

(2014), which is based on a method developed by Cottaar et al. (2012b). We assume that the intrinsic RV distribution of a single population is described by a Gaussian that is broadened by binary motions and the uncertainties in RV measurements. The RV uncertainties are calculated using equation 1 in Jeffries et al. (2014), since NGC 2547 and Gamma Vel were observed with the same instrument and processed with the same pipeline. We tried three different models: a) a single population with mean velocity RV_A and dispersion σ_A ; b) two populations, one with mean velocity RV_A , dispersion σ_A , and fraction of the total population f_A as free parameters, and a second one with a fixed mean velocity ($RV_B = 18.88$ km s $^{-1}$) and dispersion ($\sigma_B = 1.6$ km s $^{-1}$), which are the values found for Gamma Vel B by Jeffries et al. (2014); c) two populations with five free parameters (mean velocities RV_A and RV_B , dispersions σ_A and σ_B , and ratio between the two populations f_A). The most likely distributions derived by the three fits are shown in Fig. 1. The best values of the free parameters and the maximum log-likelihood are reported in Table 1. Since the models are nested, we can perform a likelihood ratio test to establish which model describes the RV distribution better. The test rejects model (a) when compared to the others with a probability > 99 per cent, while the difference in maximum log-likelihood of models (b) and (c) is not significant ($P(\ln L_{maxA} - \ln L_{maxB}) > 46$ per cent). We conclude that the RV distribution of the Li-rich members of our sample is composed of two kinematically distinct populations and that the RV distributions of NGC 2547 B and Gamma Vel B are consistent, in agreement with the initial hypothesis.

The cluster NGC 2547 (age \sim 35 Myr) is significantly older than Gamma Vel (age \sim 10-15 Myr), therefore we expect to see significant differences between the EW(Li) measured for populations A and B of NGC 2547 if the latter is associated with Gamma Vel. In Fig. 2, we plot the EW(Li) as a function of $R - I$, together with isochrones at 10, 32, and 200 Myr derived from the Baraffe et al. (1998) models. Different symbols are used for stars that – according to their RV – are associated with one of the two populations with > 80 percent confidence. As expected, in the colour range $1.0 < R - I < 1.8$, we observed very few stars belonging to NGC 2547 A, because at an age of 35 Myr they are Li-depleted, and so were excluded from our initial sample selection. However, we observed several stars belonging to NGC 2547 B in this colour range, proving that this population is younger than 35 Myr. The evidence of this age difference is supported by the presence in NGC 2547 B of a star (2MASSJ08104437-4939001) classified as a strong accretor on the basis of its $H\alpha$ emission ($EW(H\alpha)=78 \text{ \AA}$ and a line width at 10 per cent of 440 km s $^{-1}$). Such strong accretors are extremely rare in a 35 Myr old cluster, and there are none in NGC 2547 A.

In Fig. 3, we compare the two NGC 2547 populations (stars of NGC 2547 A have been selected on the basis of their RV, including Li-depleted stars) with Gamma Vel B¹. The top panel shows that the EW(Li) measured in Gamma Vel B and NGC 2547 B are consistent, suggesting that they are of similar age and younger than NGC 2547 A, because Li depletion occurs rapidly at $V - I \sim 2.5$. The bottom panel shows that Gamma Vel B and NGC 2547 B share the same locus in the CMD, which, assuming that they are coeval, suggests they are at a similar distance. The exceptions are two stars in the upper left-hand corner of the CMD, that match the sequence of NGC 2547 A. However, Li absorption cannot reliably select young (< 100 Myr) stars at $T_{\text{eff}} > 5000$ K ($V - I < 1$), so these two objects, which have RV (21.65 ± 0.19 and 23.10 ± 0.25 km s⁻¹) might be contaminating field stars or are possibly binary members of NGC 2547.

4. Discussion and conclusions

Jeffries et al. (2014) propose several scenarios to explain the presence of two populations around γ^2 Velorum, concluding that population A is the remnant of a bound cluster formed around the massive binary, and population B is a dispersed population from the wider Vela OB2 association. We have discovered 15 stars that appear to belong to Gamma Vel B and are located 2 deg (~ 10 pc, assuming a distance of ~ 340 pc) south of γ^2 Velorum, demonstrating that Gamma Vel B extends far beyond the area studied by Jeffries et al. (2014). Two scenarios might explain this result: a) the young low-mass population observed towards NGC 2547 was part of a denser cluster around γ^2 Velorum, which – after the formation of the massive binary and the expulsion of residual gas – expanded into a larger volume; b) these stars were born in a low-density diffuse environment, which also formed the other members of the Vela OB2 association.

According to the relation between cluster mass and the mass of its most massive star proposed by Weidner et al. (2010), γ^2 Velorum should be surrounded by a cluster with a mass ($\sim 1000 M_{\odot}$), which is much higher than the present total mass ($\sim 100 M_{\odot}$) estimated by Jeffries et al. (2014). It therefore seems likely that most of the original cluster that formed around the massive binary has expanded into a larger volume. Assuming that the cluster started to expand soon after the formation of the massive binary (age $\sim 5.5 \pm 1$ Myr, Eldridge 2009) and considering the intrinsic velocity dispersion of Gamma Vel B (~ 1.6 km s⁻¹), it is possible that the fastest stars formed around γ^2 Velorum have since moved ~ 10 pc. This possibility has been confirmed by recent N-body simulations aimed at investigating the origin of the two kinematically distinct populations discovered around γ^2 Velorum (Mapelli et al. 2015). Specifically, these simulations show that Gamma Vel B is supervirial and extends up to a projected distance of ~ 10 pc from the massive binary. The predicted stellar density in the outer region of the cluster is consistent with the number of stars found in NGC 2547 B. Furthermore, NGC 2547 B is only composed of low-mass stars ($R - I > 1.2$, i.e., below $\sim 0.5 M_{\odot}$). This supports the cluster expansion hypothesis, since in this scenario we should observe a higher concentration of stars in the cluster centre and mass segregation has been observed in many massive clusters (e.g., de Grijs et al. 2002).

However, not all the evidence fits this first scenario. The presence of Li-depleted stars proves that Gamma Vel is older (age $>$

10 Myr) than the massive binary. The putative expanding cluster defined by Gamma Vel B is also offset by 2 km s⁻¹ in RV from Gamma Vel A, which appears more centrally concentrated around γ^2 Velorum. Furthermore, the other early-type members of the Vela OB2 association are spread over an area of radius ~ 7 –8 degrees (~ 50 pc at a distance of 400 pc), and considering the timescale of cluster expansion, it is unlikely that they all formed in a much smaller region and spread out after the formation of the massive binary. Therefore, the second scenario seems plausible, but fails to explain why only very low-mass members of Gamma Vel B have been found towards NGC 2547 – the contrast in the distribution of Gamma Vel B and NGC 2547 B members in the bottom panel of Fig. 2 is striking.

The Gaia satellite will soon provide accurate parallaxes and proper motions (de Bruijne 2012) for the whole Vela OB2 region to $V \sim 19$. Therefore, it will be possible to perform an unbiased census of the young stellar populations and study their three-dimensional spatial and kinematic structure. This will allow us to answer this and other questions concerning the star formation process in Vela OB2 uncovered by the Gaia-ESO Survey observations.

Acknowledgements. Based on data products from observations made with ESO Telescopes at the La Silla Paranal Observatory under programme ID 188.B-3002. This work was partly supported by the European Union FP7 programme through ERC grant number 320360 and by the Leverhulme Trust through grant RPG-2012-541. We acknowledge the support from INAF and Ministero dell'Istruzione, dell'Università e della Ricerca (MIUR) in the form of the grant "Premiale VLT 2012". The results presented here are based on the work carried out during a visit at the University of Keele, and benefit from discussions held at the Gaia-ESO workshops and conferences supported by the ESF (European Science Foundation) through the GREAT Research Network Programme. LS acknowledges the support from Project IC120009 "Millennium Institute of Astrophysics (MAS)" of Iniciativa Científica Milenio del Ministerio de Economía, Fomento y Turismo de Chile

References

- Alves, J. & Bouy, H. 2012, A&A, 547, A97
 Baraffe, I., Chabrier, G., Allard, F., & Hauschildt, P. H. 1998, A&A, 337, 403
 Baumgardt, H. & Kroupa, P. 2007, MNRAS, 380, 1589
 Bressert, E., Bastian, N., Gutermuth, R., et al. 2010, MNRAS, 409, L54
 Carpenter, J. M. 2000, AJ, 120, 3139
 Claria, J. J. 1982, A&AS, 47, 323
 Cottaar, M., Meyer, M. R., Andersen, M., & Espinoza, P. 2012a, A&A, 539, A5
 Cottaar, M., Meyer, M. R., & Parker, R. J. 2012b, A&A, 547, A35
 de Bruijne, J. H. J. 2012, Ap&SS, 341, 31
 de Grijs, R., Johnson, R. A., Gilmore, G. F., & Frayn, C. M. 2002, MNRAS, 331, 228
 de Zeeuw, P. T., Hoogerwerf, R., de Bruijne, J. H. J., Brown, A. G. A., & Blaauw, A. 1999, AJ, 117, 354
 Eldridge, J. J. 2009, MNRAS, 400, L20
 Gilmore, G., Randich, S., Asplund, M., et al. 2012, The Messenger, 147, 25
 Goodwin, S. P. & Bastian, N. 2006, MNRAS, 373, 752
 Jeffries, R. D., Evans, P. A., Pye, J. P., & Briggs, K. R. 2006a, MNRAS, 367, 781
 Jeffries, R. D., Jackson, R. J., Cottaar, M., et al. 2014, A&A, 563, A94
 Jeffries, R. D., Maxted, P. F. L., Oliveira, J. M., & Naylor, T. 2006b, MNRAS, 371, L6
 Jeffries, R. D., Naylor, T., Devey, C. R., & Totten, E. J. 2004, MNRAS, 351, 1401
 Jeffries, R. D. & Oliveira, J. M. 2005, MNRAS, 358, 13
 Jeffries, R. D., Totten, E. J., & James, D. J. 2000, MNRAS, 316, 950
 Lada, C. J. & Lada, E. A. 2003, ARA&A, 41, 57
 Lanzafame, A. C., Frasca, A., Damiani, F., et al. 2015, A&A, submitted
 Lyra, W., Moitinho, A., van der Blik, N. S., & Alves, J. 2006, A&A, 453, 101
 Mapelli, M., Vallenari, A., Jeffries, R. D., et al. 2015, A&A, submitted
 Millour, F., Petrov, R. G., Chesneau, O., et al. 2007, A&A, 464, 107
 Naylor, T. & Jeffries, R. D. 2006, MNRAS, 373, 1251
 Naylor, T., Totten, E. J., Jeffries, R. D., et al. 2002, MNRAS, 335, 291
 North, J. R., Tuthill, P. G., Tango, W. J., & Davis, J. 2007, MNRAS, 377, 415
 Pasquini, L., Avila, G., Blecha, A., et al. 2002, The Messenger, 110, 1
 Pecaut, M. J. & Mamajek, E. E. 2013, ApJS, 208, 9

¹ A complete photometric catalogue in the V , R and I bands is not available for all targets in Gamma Vel or NGC 2547. Therefore not all the stars plotted in Fig. 2 are included in Fig. 3 and vice-versa.

- Pettersson, B. 2008, in Handbook of Star Forming Regions, Volume II, ed. Reipurth, B., 43
- Randich, S. & Gilmore, G. 2013, *The Messenger*, 154, 47
- Sahu, M. S. 1992, PhD thesis, Kapteyn Institute, Postbus 800 9700 AV Groningen, The Netherlands
- Shobbrook, R. R. 1986, *MNRAS*, 220, 825
- Siess, L., Dufour, E., & Forestini, M. 2000, *A&A*, 358, 593
- van Leeuwen, F. 2009, *A&A*, 497, 209
- Weidner, C., Kroupa, P., & Bonnell, I. A. D. 2010, *MNRAS*, 401, 275
- Wright, N. J., Parker, R. J., Goodwin, S. P., & Drake, J. J. 2014, *MNRAS*, 438, 639

-
- ¹ INAF-Osservatorio Astrofisico di Arcetri, Largo E. Fermi, 5, 50125, Firenze, Italy
- ² Astrophysics Group, Research Institute for the Environment, Physical Sciences and Applied Mathematics, Keele University, Keele, Staffordshire ST5 5BG, United Kingdom
- ³ Institute of Astronomy, ETH Zurich, Wolfgang-Pauli-Strasse 27, 8093 Zurich, Switzerland
- ⁴ INAF-Osservatorio Astronomico di Padova, Vicolo dell'Osservatorio 5, I35122, Padova
- ⁵ Instituto de Astrofísica de Andalucía-CSIC, Apdo. 3004, 18080, Granada, Spain
- ⁶ Dipartimento di Fisica e Chimica, Università di Palermo, Piazza del Parlamento 1, 90134, Palermo, Italy
- ⁷ INAF - Osservatorio Astronomico di Palermo, Piazza del Parlamento 1, 90134, Palermo, Italy
- ⁸ INAF - Osservatorio Astrofisico di Catania, via S. Sofia 78, 95123, Catania, Italy
- ⁹ Dipartimento di Fisica e Astronomia, Sezione Astrofisica, Università di Catania, via S. Sofia 78, 95123, Catania, Italy
- ¹⁰ Instituto de Física y Astronomía, Universidad de Valparaíso, Av. Gran Bretaña 1111, Valparaíso, Chile
- ¹¹ Depto. de Astrofísica, Centro de Astrobiología (CSIC-INTA), ESAC campus, 28691, Villanueva de la Cañada, Madrid, Spain
- ¹² Suffolk University, Madrid Campus, C/ Valle de la Viña 3, 28003, Madrid, Spain
- ¹³ Institute of Astronomy, University of Cambridge, Madingley Road, Cambridge CB3 0HA, United Kingdom
- ¹⁴ Instituto de Astrofísica de Canarias, E-38205 La Laguna, Tenerife, Spain
- ¹⁵ European Southern Observatory, Alonso de Cordova 3107 Vitacura, Santiago de Chile, Chile
- ¹⁶ Astrophysics Research Institute, Liverpool John Moores University, 146 Brownlow Hill, Liverpool L3 5RF, United Kingdom
- ¹⁷ Millennium Institute of Astrophysics, Av. Vicuña Mackenna 4860, 782-0436 Macul, Santiago, Chile